Clustering of impurity atoms in Co-doped anatase TiO_2 thin films probed with soft x-ray fluorescence

2006 J. Phys.: Condens. Matter 18 4243

(http://iopscience.iop.org/0953-8984/18/17/012)

INSTITUTE OF PHYSICS PUBLISHING JOURNAL OF PHYSICS: CONDENSED MATTER

J. Phys.: Condens. Matter **18** (2006) 4243–4251 doi:10.1088/0953-8984/18/17/012

Clustering of impurity atoms in Co-doped anatase TiO_2 thin films probed with soft x-ray fluorescence

G S Chang[1], E Z Kurmaev[2], D W Boukhvalov[2], L D Finkelstein[2], D H Kim[3,4], T-W Noh[3], A Moewes[1] and T A Callcott[5]

[1] Department of Physics and Engineering Physics, University of Saskatchewan, 116 Science Place, Saskatoon, SK, S7N 5E2, Canada
[2] Institute of Metal Physics, Russian Academy of Sciences-Ural Division, Yekaterinburg GSP-170, Russia
[3] School of Physics and Research Center for Oxide Electronics, Seoul National University, Seoul 151-747, Korea
[4] Condensed Matter Sciences Division, Oak Ridge National Laboratory, Oak Ridge, TN 37830, USA
[5] Department of Physics and Astronomy, University of Tennessee, Knoxville, TN 37996, USA

E-mail: gapsoo.chang@usask.ca

Received 14 December 2005
Published 13 April 2006
Online at stacks.iop.org/JPhysCM/18/4243

Abstract

The electronic structure of Co-doped anatase TiO_2 epitaxial thin films grown at different partial oxygen pressures is investigated using soft x-ray emission spectroscopy. The resonantly excited Co $L_{2,3}$ x-ray emission spectra of ferromagnetic $Ti_{0.96}Co_{0.04}O_2$ samples for the oxygen-deficient regime show that the ratio of integral intensities for Co L_2 and L_3 emission lines significantly decreases with respect to nonmagnetic samples in the oxygen-rich regime. This is due to $L_2L_3M_{4,5}$ Coster–Kronig transitions and suggests that ferromagnetic $Ti_{0.96}Co_{0.04}O_2$ samples have n-type charge carriers and Co–Co bonds between substitutional and interstitial Co atoms are present while Co–O bonds are dominant in nonmagnetic $Ti_{0.96}Co_{0.04}O_2$ samples in the oxygen-rich regime. Electronic structure calculations show that the presence of free charge carriers and Co segregation play a crucial role in strong ferromagnetism at room temperature in Co-doped TiO_2.

1. Introduction

Diluted magnetic semiconductors (DMSs) have been studied extensively because of their potential application to spintronic devices in which carriers are provided and their charge and spin are manipulated. Previous research has focused on two types of DMS families: II–VI semiconductors, such as Mn-doped CdTe and ZnSe, and III–V semiconductors, for example Mn-doped GaAs [1, 2]. The latter material has especially attracted great attention since it becomes a ferromagnetic DMS with a Curie temperature (T_C) of 110 K [2]. However, practical

Table 1. Synthesis parameters of $Ti_{0.96}Co_{0.04}O_2$ samples.

Sample	Composition	Partial O_2 pressure (Torr)	Thickness (nm)	Property
1	$Ti_{0.96}Co_{0.04}O_{2-\delta}$[a]	1.0×10^{-6}	40	Ferromagnetic
2	$Ti_{0.96}Co_{0.04}O_{2-\delta}$	3.5×10^{-6}	40	Ferromagnetic
3	$Ti_{0.96}Co_{0.04}O_{2-\delta}$	1.0×10^{-4}	30	Nonmagnetic

[a] δ varies with oxygen partial pressure.

spintronic devices require new materials with higher T_C in order to allow electrons and holes of well defined and long-lived spin states to be controlled at ambient temperature. It has been found recently that Co-doped 3d oxides such as ZnO:Co, $SnO_{2-\delta}$:Co, Cu_2O:Co, and TiO_2:Co show ferromagnetic behaviour at room temperature (RT) [3–6]. These findings have generated strong interest in the DMS community because they could allow us to create new multifunctional oxides with spin-polarized carriers. Among these dilute magnetic oxides, Co-doped anatase TiO_2 is considered to be the most magnetically robust DMS with regard to its large magnetic moment (1.26 μ_B per Co atom), large remanent magnetization (30%), and high T_C (at least 400 K) [7, 8].

According to references [7] and [8], the ferromagnetic ordering of Co ions in $Co_xTi_{1-x}O_2$ strongly depends on the presence of excess oxygen vacancies and originates from substitutional Co^{2+} impurities magnetically coupled with conduction electrons that are induced by oxygen vacancies. Since the growth conditions on the other hand significantly affect the magnetic properties of TiO_2:Co [7], the possibility of Co segregation (Co clustering) cannot be excluded in this system. The presence of such clusters was revealed by cross-sectional transmission electron microscopy (TEM) [9, 10]. If the material is grown under less oxidizing conditions, these clusters become more pronounced and the magnetic moment becomes similar to that of bulk Co metal (1.75 μ_B/Co) [11]. More evidence for Co clustering has been found from transport measurements. It has been shown that the resistivity of TiO_2:Co follows a $\log(\rho) \sim T^{-1/2}$ correlation over a wide temperature range. This is considered typical for metallic clusters embedded in a dielectric matrix [12, 13].

In the present paper, we show that resonant inelastic x-ray scattering (RIXS) provides a powerful way to probe local ordering change in magnetic dopants and to monitor the presence of free charge carriers in DMS systems. The experimental results and relevant theoretical calculation are discussed to verify the relation of local order change and free charge carrier to ferromagnetism in Co-doped TiO_2 at RT.

2. Experimental details

High quality epitaxial films of $Ti_{0.96}Co_{0.04}O_{2-\delta}$ (δ varies with partial oxygen pressure) were grown on $SrTiO_3$(001) single crystalline substrates using a pulsed laser deposition method as described elsewhere [9, 11]. A sintered polycrystalline $Ti_{0.96}Co_{0.04}O_2$ target was ablated by a KrF excimer laser with a fluence of 1.5 J cm^{-2} at 2 Hz. The substrate temperature was kept constant at 650 °C and the partial oxygen pressure (P_{O_2}) was varied from 1×10^{-6} to 1×10^{-4} Torr. The growth rate was less than 0.2 nm min^{-1}. The thickness of each film was determined from oscillations in the x-ray reflectivity to be about 30–40 nm (see table 1). The XRD pattern reveals the crystal structure of TiO_2 and does not exhibit features from traces of metallic Co. According to the magnetic hysteresis measurements of the samples (using a superconducting quantum interference device), only $Ti_{0.96}Co_{0.04}O_{2-\delta}$ films grown under P_{O_2}

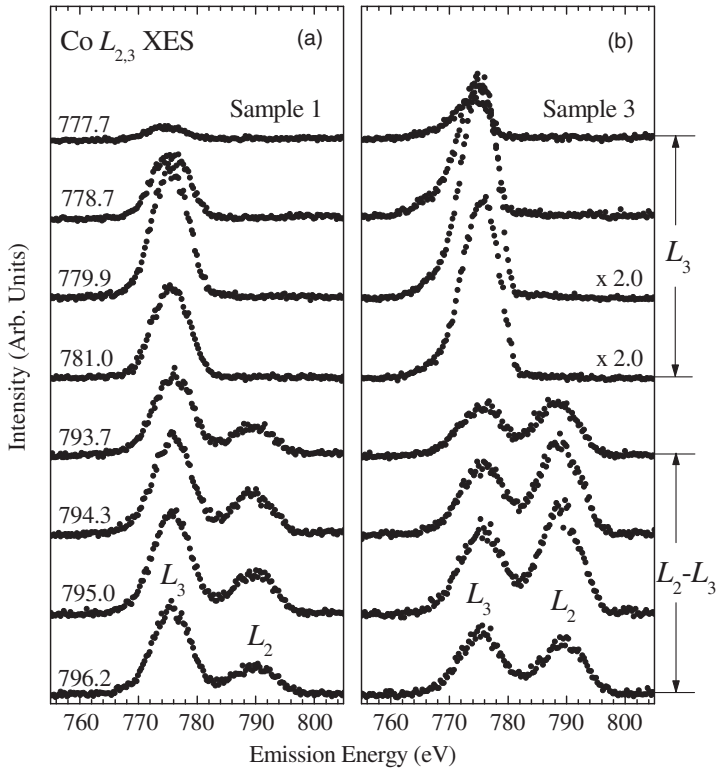

Figure 1. Co $L_{2,3}$ XES spectra of oxygen-deficient $Ti_{0.96}Co_{0.04}O_2$ sample 1 (a) and oxygen-rich sample 3 (b).

below 1×10^{-5} Torr (samples 1 and 2 in the oxygen-deficient regime) exhibit ferromagnetism at RT. The film grown at a pressure P_{O_2} of 1×10^{-4} Torr is nonmagnetic (sample 3 in the oxygen-rich regime) [9].

The x-ray emission spectroscopy (XES) measurements were carried out at beamline 8.0.1 of the Advanced Light Source at Lawrence Berkeley National Laboratory. Resonant Co $L_{2,3}$ ($3d4s \rightarrow 2p$ transition), Ti $L_{2,3}$ ($3d4s \rightarrow 2p$ transition) and nonresonant O Kα ($2p \rightarrow 1s$ transition) emission spectra were recorded at RT and only Co emission spectra reveal noticeable changes in dependence on partial oxygen pressure P_{O_2}. All measured spectra are normalized to the number of photons falling on the sample monitored by a highly transparent gold mesh.

3. Results and discussion

Co $L_{2,3}$ XES spectra of ferromagnetic (sample 1) and nonmagnetic $Ti_{0.96}Co_{0.04}O_2$ films (sample 3) measured at different excitation energies (E_{exc}) are presented in figure 1. The two main bands located around 775 and 790 eV correspond to Co L_3 ($3d4s \rightarrow 2p_{3/2}$ transition) and Co L_2 ($3d4s \rightarrow 2p_{1/2}$ transition) normal emission lines, respectively. Their energy separation exactly corresponds to spin–orbital splitting of Co 2p and does not change with excitation energy. We note that the integral intensity ratio of Co L_2 to L_3 emission lines ($I(L_2)/I(L_3)$) of sample 1 excited above the L_2 threshold (spectra for 793.7 eV $\leqslant E_{exc} \leqslant$ 796.2 eV) is

significantly smaller than that of sample 3. In the case of sample 2 (not shown), the overall spectral behaviour is similar to that of sample 1. The differences in the Co $L_{2,3}$ XES spectra of ferromagnetic and nonmagnetic $Ti_{0.96}Co_{0.04}O_2$ samples reflect changes in the number of free charge carriers for different partial oxygen pressures P_{O_2} during sample synthesis and are discussed below.

L_2 and L_3 x-ray emission from 3d elements corresponds to x-ray transitions from (occupied) 3d4s valence states to $2p_{1/2}$ and $2p_{3/2}$ core vacancies. For free atoms with fully occupied d shell, the relative intensity ratio of L_2 and L_3 XES lines, $I(L_2)/I(L_3)$, is determined only by the statistical population of $2p_{1/2}$ and $2p_{3/2}$ levels and therefore should be equal to $1/2$ if no radiationless transitions occur. In solids this ratio can deviate from the value of $1/2$ due to the electrostatic interaction between 2p core holes and electrons in the unfilled 3d shell. In any case the integral intensity ratio $I(L_2)/I(L_3)$ can provide information about the population of the valence bands (with d symmetry).

Aside from the 2p–3d interaction, radiationless $L_2L_3M_{4,5}$ Coster–Kronig (C–K) transitions also influence the intensity ratio $I(L_2)/I(L_3)$ in solids. Generally, C–K transitions partially depopulate the L_2 states of the system when radiationless transitions from the L_2 to the L_3 level occur before the emission process can take place. In this case the transition energy can be released via emission of 3d Auger electrons. The probability for this process in free atoms is small but it is strongly enhanced in condensed matter systems. This is due to the fact that a screening of intra-atomic electron interactions in solids leads to a decrease in energy difference between initial and final states of the radiationless C–K process. This effect becomes particularly prominent in metals [14, 15].

Taking into account all these factors, we used the following expression for the $I(L_2)/I(L_3)$ ratio [16]:

$$\frac{I(L_2)}{I(L_3)} = \frac{1 - f_{2,3}}{f_{2,3} + \mu_3/\mu_2}, \tag{1}$$

where $f_{2,3}$ is the probability for the C–K process and μ_3/μ_2 is the ratio of total photoabsorption coefficients for excitation energies at L_3 and L_2 threshold. In the case of excitation energy well above the L_2 threshold (nonresonant regime), μ_3/μ_2 has a constant value of two for all elements. Therefore, the ratio $I(L_2)/I(L_3)$ is determined only by the parameter $f_{2,3}$, which increases for a given element (Co in our case) with the number of free d carriers available [15]. For resonant excitation, on the other hand, the parameter μ_3/μ_2 changes (with E_{exc}) and becomes minimal when exciting at the L_2 threshold [16]. This means that the ratio $I(L_2)/I(L_3)$ strongly increases excitation at the L_2 threshold (795 eV for $Ti_{0.96}Co_{0.04}O_{2-\delta}$).

To verify the influence of radiationless $L_2L_3M_{4,5}$ C–K transitions for nonresonant and resonant excitation, we compare Co $L_{2,3}$ XES spectra of the samples nonresonantly excited at 820 eV (well above L_2 edge) to emission spectra resonantly excited at 795 eV (L_2 threshold) in figure 2. The ratio $I(L_2)/I(L_3)$ for the nonmagnetic sample 3 (oxygen-rich regime) strongly depends on E_{exc}, indicating that $L_2L_3M_{4,5}$ C–K transitions are strongly suppressed due to a lack of free charge carriers and thus the change in the intensity ratio $I(L_2)/I(L_3)$ is largely governed by μ_3/μ_2. On the other hand, the ratio $I(L_2)/I(L_3)$ is reduced for samples 1 and 2 (oxygen-deficient regime) compared to that of the oxygen-rich sample 3 for both nonresonant and resonant excitation and also shows less correlation with excitation energy. This shows that C–K transitions are significantly enhanced by a larger number of 3d conduction electrons in samples 1 and 2. A similar tendency is found in the XES spectra of metallic Co and dielectric CoO, which are displayed in figure 3. We note that the full width at half maximum (FWHM) of Co $L_{2,3}$ XES spectra of samples 1–3 is larger than that of the Co and CoO reference samples displayed in figure 3. Due to the small concentration of Co dopants in $Ti_{0.96}Co_{0.04}O_2$, the

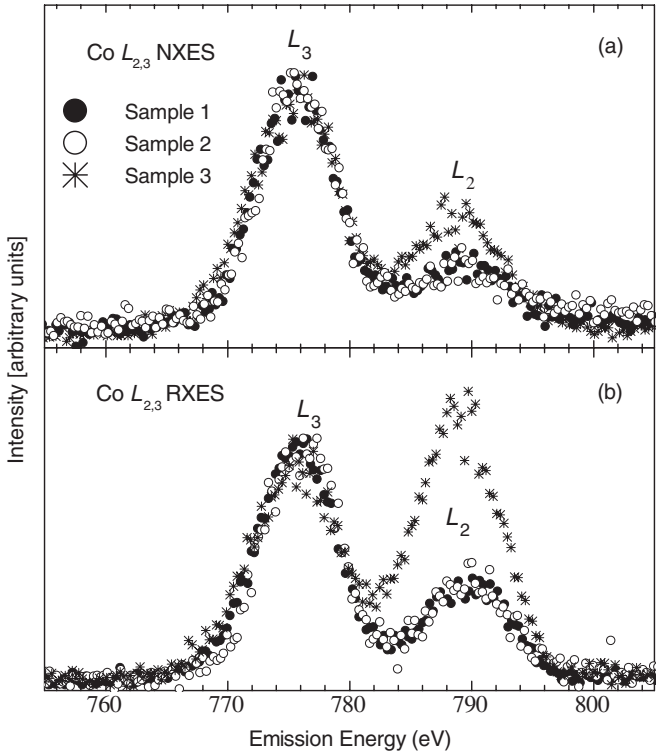

Figure 2. Co $L_{2,3}$ XES spectra of samples 1–3 excited nonresonantly (E_{exc} = 820 eV) (a) and resonantly at the L_2 threshold (E_{exc} = 795 eV) (b). Different synthesis parameters for the three samples are given in table 1.

spectrometer entrance slit had to be opened in order to collect a sufficient number of photons, giving rise to a decreased spectrometer resolution for $Ti_{0.96}Co_{0.04}O_2$.

When comparing to the spectra of the Co and CoO reference samples, we find that the Co $L_{2,3}$ XES spectra of the nonmagnetic sample 3 are very similar to those of CoO. This similarity is not surprising because Co dopants substituting Ti atoms in the TiO_2 lattice are surrounded by oxygen (in octahedral coordination). It should be noted that x-ray transitions in the x-ray emission process occur within the Co atom and thus the corresponding XES spectra are determined mainly by the first coordination sphere of the excited atom. On the other hand the Co $L_{2,3}$ XES spectra of ferromagnetic samples 1 and 2 are more similar to the XES spectra of Co metal than to those of CoO. However, as shown in table 2, the intensity ratio $I(L_2)/I(L_3)$ for samples 1 and 2 is slightly larger than that of Co metal. This means that both Co–Co and Co–O bonds coexist in ferromagnetic $Ti_{0.96}Co_{0.04}O_2$, while in the nonmagnetic samples Co–O bonds are much more dominant. We therefore suppose changes in the local ordering of $Ti_{0.96}Co_{0.04}O_2$ films due to a segregation of Co atoms in interstitial sites from Co–Co interaction near the excited Co atom. Since such changes in local ordering depend on the partial oxygen pressure P_{O_2} and are not accompanied by formation of additional phases, only a chemically sensitive local-probe method like XES provides an efficient analysis.

In addition to $L_2L_3M_{4,5}$ C–K transitions, the $L_3M_1M_{4,5}$ and $L_3M_{2,3}M_{4,5}$ Auger transitions can also affect the intensity of resonantly excited Co L_3 XES spectra (spectra for excitation energies between 777.7 and 781.0 eV in figure 1). This occurs when a hole is transferred from

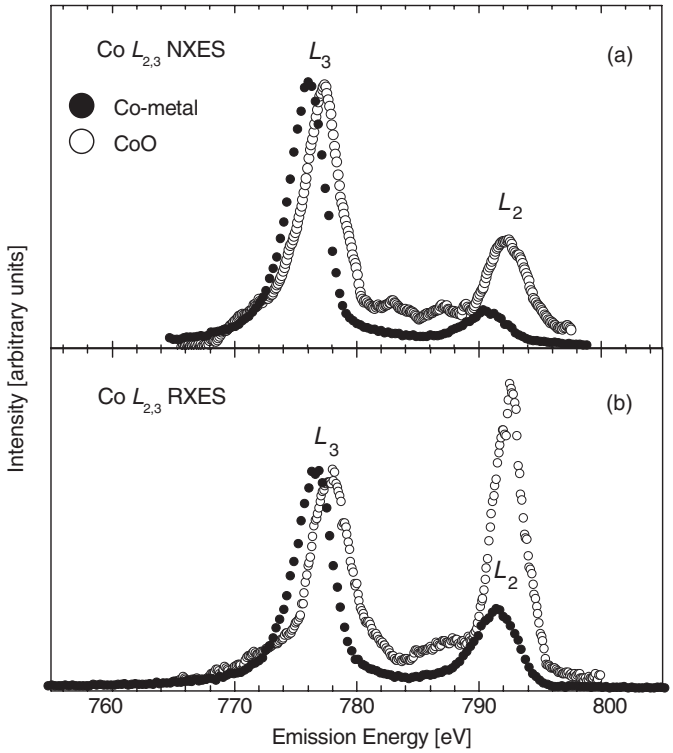

Figure 3. Co $L_{2,3}$ XES spectra of Co and CoO samples excited nonresonantly ($E_{exc} = 820$ eV) (a) and resonantly at the L_2 threshold ($E_{exc} = 795$ eV) (b).

Table 2. $I(L_2)/I(L_3)$ intensity ratio of $Ti_{0.96}Co_{0.04}O_{2-\delta}$ samples (samples 1–3) and reference samples.

Sample	Nonresonant spectra	Resonant spectra
1	0.306	0.388
2	0.306	0.388
3	0.513	1.163
CoO	0.439	1.408
Co	0.160	0.352

the L_3 to the M_1 or $M_{2,3}$ level accompanied by collective plasma vibrations. At the plasma vibration energy of about 10–15 eV the optical potential reaches its maximum value and only depends on the concentration of the conducting electrons [17]. It is important to note that this energy coincides with the spin–orbit energy when an L_2 hole relaxes to the L_3 level. This relaxation energy is transferred to the electron density, giving rise to plasma vibrations.

The above considerations of resonantly excited Co $L_{2,3}$ emission lines and their intensity ratio $I(L_2)/I(L_3)$ provide direct evidence that $Ti_{0.96}Co_{0.04}O_2$ films that show ferromagnetic properties have not only Co–O but also significant Co–Co interaction. This supports the existence of precipitated Co atoms leading to large numbers of free charge carriers (in the form of conduction band electrons with d symmetry). When $Ti_{0.96}Co_{0.04}O_2$ films are grown under high oxygen pressure, Co atoms mostly substitute for Ti atoms and thus interact strongly

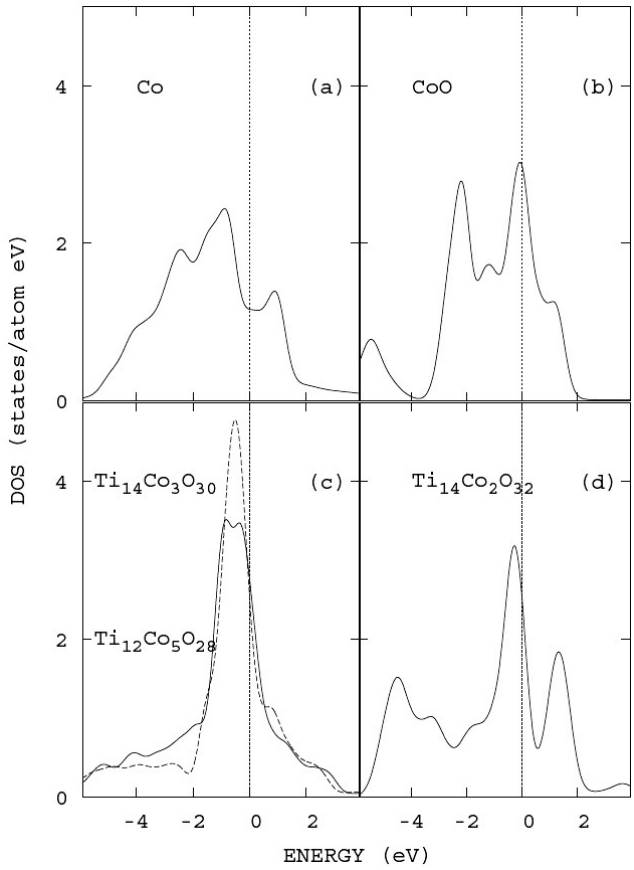

Figure 4. Calculated Co 3d DOS for Co metal (a), CoO (b), and two model configurations of TiO_2:Co with interstitial Co in the oxygen-deficient regime (c) and that in the oxygen-rich regime (d).

with the surrounding oxygen octahedron for the oxygen-rich sample. In this case, the system is lacking free charge carriers and does not exhibit ferromagnetic properties.

Recently, there have been several theoretical papers on the significant effects of the structural disorder and cluster formation of 3d dopants on ferromagnetism in some DMS compounds. These results are based on using mean-field theory [18, 19] and density functional theory [20]. In accordance with these approaches used, electronic structure and exchange interactions for different configurations of Co dopants within a supercell containing 64 tetragonal units ($4a \times 4a \times 4c$) of anatase TiO_2 were investigated using the linearized muffin-tin-orbital method in the atomic-sphere approximation (LMTO-ASA) with the local spin-density approximation (LSDA)[6] [22]. An anatase $Ti_{14}Co_2O_{32}$ structure with two substitutional Co atoms [Co(S)] was calculated first in order to simulate super-exchange interaction with oxygen participation. The calculated density of states (DOS) of the $Ti_{14}Co_2O_{32}$ model structure is displayed in figure 4 and is found to be similar to that of CoO (see figures 4(b) and (d)).

In addition, the exchange interaction parameters between Co impurities were determined by using a similar method described in [23] which does not require a total energy calculation.

[6] We have used the same abbreviation and structural parameters for clusters as in the paper of Geng and Kim [21].

This is a very efficient method for calculating such a large system containing more than 50 atoms, without having to make small corrections to the total energy. The resulting exchange interactions between two Co(S) atoms via oxygen result in a T_C value of about 140 K and thus is not strong enough to induce ferromagnetism at RT. Taking into account the XES results, two different types of Co configurations in TiO_2 are calculated: $Ti_{14}Co_3O_{30}$ with two Co(S) and one interstitial Co atom (Co(I)) (see [21]) and $Ti_{12}Co_5O_{28}$ with four Co(S) and one Co(I) ion, which simulates the local structure of Co atoms in oxygen-deficient TiO_2:Co. The choice of such clusters is based on previous electronic structure calculations of Co dopants and defects in anatase TiO_2 [21, 24]. Figures 4(a) and (c) show that the Co 3d DOS for both clusters is similar to the DOS of Co metal rather than the DOS of CoO, and therefore these configurations are good models for Co clusters in the oxygen-deficient case.

According to our calculations, the super-exchange interaction between Co(S) and Co(I) (or $J_{Co(S)-Co(I)}$) is much stronger than the one for Co(S) and Co(S) (or $J_{Co(S)-Co(S)}$). In the case of a model cluster with a 2Co(S) + Co(I) configuration, $J_{Co(S)-Co(I)}$ has a value of about 280 K and is still too weak to induce ferromagnetism (at room temperature). However, for the cluster with 4Co(S) + Co(I) configuration, $J_{Co(I)-Co(S)}$ significantly increases and free conduction electrons begin to be present. The amount of free charge depends on the degree of oxygen deficiency and plays an important role in increasing $J_{Co(I)-Co(S)}$. The additional exchange interaction due to free charge carriers in a strongly oxygen-deficient configuration enhances $J_{Co(S)-Co(I)}$ up to 650 K, which is much higher than the value of 225 K obtained for the same kind of cluster in the oxygen-rich configuration. From these exchange values we can calculate T_C for an embedded cluster using a standard formula for the Ising model:

$$T_C = \sum_{i=1}^{N} \frac{JS(S+1)}{3k_B}, \tag{2}$$

where N is the total number of exchange pairs, and S is the spin on the magnetic atoms. The resulting T_C value that corresponds to a $J_{Co(S)-Co(I)}$ of 650 K is about 347 K, which is very close to the experimental result.

In addition, the magnetic moments of Co(S) and Co(I) calculated for TiO_2:Co with the oxygen-deficient configuration are about 0.7 and 1.65 μ_B, respectively. The average magnetic moment of 1.2 μ_B per Co atom is in good agreement with the experimental value of 1.26 μ_B [7, 8]. Based on these results we suggest that the presence of interstitial Co atoms and the relevant Co cluster consisting of a sufficient number of substitutional and interstitial Co atoms must be taken into account to induce ferromagnetism in TiO_2:Co (at room temperature). It is noted that these calculated results describe only the magnetic characteristics of Co clusters in TiO_2 and not of the entire system because they provide information only on short-range ferromagnetism. The correlation between short- and long-range ferromagnetism is still an open problem for high T_C ferromagnetism of the DMS systems.

4. Conclusions

We have shown that RIXS can be used to probe the local ordering changes in Co-doped TiO_2 films grown at different partial oxygen pressure. By monitoring the intensity ratio $I(L_2)/I(L_3)$ of nonresonantly and resonantly excited Co $L_{2,3}$ emission spectra, it is found that n-type charge carriers are induced in oxygen-deficient TiO_2:Co showing the ferromagnetic property at RT. From our spectroscopic measurements and electronic structure calculations we find that two things play a crucial role: (1) the presence of direct Co(S)–Co(I) interaction due to segregation of Co dopants into interstitial sites and (2) the presence of free charge carriers, that enhances super-exchange interaction and induces strong ferromagnetism in these materials.

Moreover, the calculated magnetic properties of the Co configuration that consists of four substitutional and one interstitial Co atom agree with the experimental results for ferromagnetic Co-doped TiO_2.

Acknowledgments

This work is supported by the Natural Sciences and Engineering Research Council of Canada (NSERC), the Canada Research Chair programme, the KOSEF through CSCMR, and the Korean Ministry of Science and Technology through the Creative Research Initiative programme. We gratefully acknowledge the Research Council of the President of the Russian Federation (grants NSH-1026.2003.2 and NSH-4640.2006.2), the Russian Science Foundation for Basic Research (projects 05-02-16438 and 05-02-17704) and RFBR-Ural (project 04-02-96096).

References

[1] Furdyna J K and Kossut J 1988 *Diluted Magnetic Semiconductors, Semiconductors and Semimetals* vol 25 (New York: Academic)
[2] Ohno H 1998 *Science* **281** 951
[3] Lim S-W, Hwang D-K and Myoung J-M 2003 *Solid State Commun.* **125** 231
[4] Ogale S B, Choudhary R J, Buban J P, Lofland S E, Shinde S R, Kale S N, Kulkarni V N, Higgins J, Lanci C, Simpson J R, Browning N D, Das Sarma S, Drew H D, Greene R L and Venkatesan T 2003 *Phys. Rev. Lett.* **91** 077205
[5] Kale S N, Ogale S B, Shinde S R, Sahasrabuddhe M, Kulkarni V N, Greene R L and Venkatesan T 2003 *Appl. Phys. Lett.* **82** 2100
[6] Matsumoto Y, Murakami M, Shono T, Hasegawa T, Fukumura T, Kawasaki M, Ahmet P, Chikyow T, Koshihara S and Koinuma H 2001 *Science* **291** 854
[7] Chambers S A 2002 *Mater. Today* **5** 34
[8] Chambers S A, Thevuthasan S, Farrow R F C, Marks R F, Thiele J U, Folks L, Samant M G, Kellock A J, Ruzycki N, Ederer D L and Diebold U 2001 *Appl. Phys. Lett.* **79** 3467
[9] Kim D H, Yang J S, Lee K W, Bu S D, Noh T W, Oh S-J, Kim Y-W, Chung J-S, Tanaka H, Lee H Y and Kawai T 2002 *Appl. Phys. Lett.* **81** 2421
[10] Chambers S A, Droubay T, Wang C M, Lea A S, Farrow R F C, Folks L, Deline V and Anders S 2003 *Appl. Phys. Lett.* **82** 1257
[11] Kim J-Y, Park J-H, Park B-G, Noh H-J, Oh S-J, Yang J S, Kim D-H, Bu S D, Noh T-W, Lin H-J, Hsieh H-H and Chen C T 2003 *Phys. Rev. Lett.* **90** 017401
[12] Kennedy R J, Stampe P A, Hu E, Xiong P, von Molnár S and Xin Y 2004 *Appl. Phys. Lett.* **84** 2832
[13] Sheng P, Abeles B and Arie Y 1973 *Phys. Rev. Lett.* **31** 44
[14] Krause M O 1979 *J. Phys. Chem. Ref. Data* **8** 307
[15] Grebennikov V I 2002 *Surface Investigations: X-ray, Synchrotron and Neutron Techniques* **11** 41
[16] Kurmaev E Z, Ankudinov A L, Rehr J J, Finkelstein L D, Karimov P F and Moewes A 2005 *J. Electron Spectrosc. Relat. Phenom.* **148** 1
[17] Grebennikov V I 2000 *Phys. Met. Metallogr.* **89** 425
[18] Berciu M and Bhatt R N 2001 *Phys. Rev. Lett.* **87** 107203
[19] Xu J L, van Schilfgaarde M and Samolyuk G D 2005 *Phys. Rev. Lett.* **94** 097201
[20] Cui X Y, Medvedeva J E, Delley B, Freeman A J, Newman N and Stampfl C 2005 *Phys. Rev. Lett.* **95** 256404
[21] Geng W T and Kim K S 2004 *Solid State Commun.* **129** 741
[22] Andersen O K 1975 *Phys. Rev.* B **12** 3060
[23] Anisimov V I, Aryasetiawan F and Lichtenstein A I 1997 *J. Phys.: Condens. Matter* **9** 767
[24] Sullivan J M and Erwin S C 2003 *Phys. Rev.* B **67** 144415